ELSEVIER

Earth and Planetary Science Letters 205 (2003) 273–280

EPSL

www.elsevier.com/locate/epsl

Experimental evidence of transformation plasticity in silicates: minimum of creep strength in quartz

Christian Schmidt *, David Bruhn, Richard Wirth

GeoForschungsZentrum Potsdam, Telegrafenberg, 14473 Potsdam, Germany

Received 5 July 2002; received in revised form 25 September 2002; accepted 14 October 2002

Abstract

Mechanical weakening due to solid state transformation of mineral phases has long been proposed to be a significant mechanism for localization of deformation in the Earth's lithosphere and the mantle transition zone. However, experimental observations confirming such a proposition are lacking. Here we present a novel approach to prove the existence of a minimum in the creep strength of quartz at the α–β transition by observing the deformation of fluid inclusions in a quartz crystal using a hydrothermal diamond-anvil cell. Pressure differences required for permanent deformation of the quartz around fluid inclusions were significantly lower at the phase transition than in either the stability fields of α- or β-quartz. These results indicate that transformation plasticity of silicates can indeed cause a considerable localized reduction in the strength of the Earth's crust and mantle.

Keywords: fluid inclusions; deformation; plastic flow; diamond-anvil cell; phase transition

1. Introduction

One of the key problems in our understanding of the dynamics of the Earth's interior is how and why deformation of the ductile lithosphere becomes concentrated in narrow shear zones. An important localization mechanism that has long been proposed for the Earth's crust and mantle is weakening due to solid state transformation of mineral phases, often referred to as 'transformation plasticity' [1–4]. However, unequivocal experimental evidence of this process in geologically relevant materials is still lacking [5]. In Earth sciences, one of the most intensively studied phase transformations is the α–β transition of quartz, which is the mineral often used to represent the strength of the continental crust [6]. While minima in the elastic strength at the transition are well documented experimentally [7,8], there is no evidence of analogous behavior in plastic deformation [5,9]. Significant mechanical weakening due to transformation plasticity has been reported for other materials, such as several metallic systems [10,11], some ionic crystals [12] and oxides including ice [13]. However, despite numerous studies of the creep behavior of quartz [14,15], the effect of the α–β transition on plastic deformation is not well understood.

The few experimental constraints on the effect

* Corresponding author. Tel.: +49-331-288 1406; Fax: +49-331-288 1402.
E-mail address: hokie@gfz-potsdam.de (C. Schmidt).

0012-821X/02/$ – see front matter
PII: S0012-821X(02)01046-4

of the α–β transition on the creep behavior of quartz include data for wet synthetic quartz single crystals (900 H/10^6 Si) at 140 MPa axial stress [16], which show a sharp offset in the activation energy for creep at the transition, with much lower activation energies for β-quartz. Other experimental studies show a maximum in the compliance in axial compression tests at the transition, but no permanent deformation after decompression [7]. In three-point bending tests of quartz single crystals some irreversible deformation, albeit very small, was achieved by cycling across the α–β transition temperature [9], but there is no evidence that deformation was caused by a local minimum of creep strength at the transition temperature; it might simply be due to a relative weakness of β-quartz with respect to α-quartz.

Observation of deformation at the α–β transition of quartz in standard axial compression/extension experiments is complicated because of a simultaneous peak in thermal expansion. Thermal expansion overprints the potential effect of deformation at the transition temperature, which is usually detected by the relative displacement of two reference points. Thus any deformation measured after the experiment cannot unequivocally be linked with the transformation. We therefore applied a new experimental approach that allows direct observation of both phase transformation and deformation in situ.

2. Experimental approach

The apparatus used is a hydrothermal diamond-anvil cell (HDAC), in which temperature is well defined and thermal gradients within the sample are small. The pressure medium is water, which provides a hydrostatic confining pressure around the sample [17]. The confining pressure increases with temperature (Fig. 1) and can be calculated accurately from the equation of state of water [18] and from the temperature of the α–β transition of the quartz sample [19]. The advantage of using a HDAC to observe transformation plasticity is that samples can be monitored optically in situ at high temperature and pressure. The α–β transition in the quartz sample is recognized by a rapid change of the interference colors in polarized light. However, the HDAC is not designed to perform standard deformation experiments.

To circumvent this problem we used samples with synthetic fluid inclusions [20,21] for our experiments. Stress in the sample is created around the inclusions if the confining pressure P_c differs from the pressure in the inclusion P_i. P_c and P_i are determined as explained in detail in Fig. 1. The stress in the mineral around the inclusion is proportional to the pressure difference $P_c - P_i$ and the plastic strain is proportional to the irreversible change in the inclusion volume. By decreasing the volume of the inclusion, the fluid pressure P_i in the inclusion is increased, which in turn reduces the pressure difference $P_c - P_i$ and the stress, the driving force of deformation. This reduction in pressure difference slows down the rate of deformation around the inclusions.

It is well known that such changes of the fluid inclusion volume can occur even at laboratory timescales and can be recognized by a distinct change in inclusion shape and density [22,23]. Permanent deformation of fluid inclusions has been observed in the stability fields of both α- and β-quartz [22]. Microstructural investigations by transmission electron microscopy (TEM) reveal a high dislocation density around deformed inclusions [23], which is interpreted as clear evidence of plastic deformation. However, these observations were made after long-term experiments (30–180 days) using cold-seal pressure vessels, which do not permit in situ observation of the sample, such that the effect of the phase transition could not be studied. The essence of our approach is to observe in situ at which pressure and temperature such a change in shape and density of the fluid inclusions occurs and how it relates to the phase transformation of quartz.

Our samples were 80 μm thin disks with a diameter of 200–300 μm cut from a single crystal Brazilian quartz (Fig. 2A), which contained synthetically introduced pure water inclusions of well-defined density. The fluid inclusion synthesis followed the procedure described in [20]. Starting materials were distilled water and a prefractured quartz core. The core was cut from an inclusion-

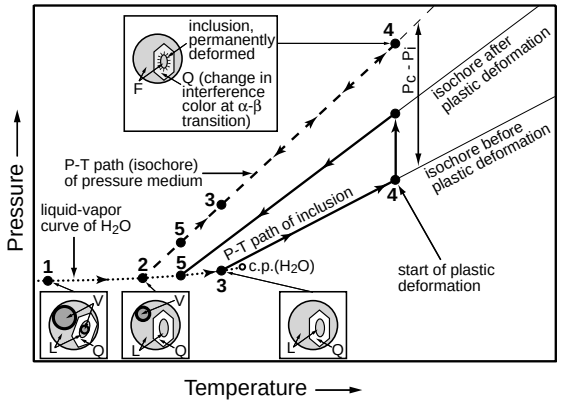

Fig. 1. Schematic diagram showing the pressure–temperature paths of the pressure medium and of an inclusion in quartz during a deformation experiment. The insets show schematic plan views of the sample chamber through the diamond windows of the HDAC at specific points along the paths. The sequence of an experimental run is indicated by the numbers 1 to 5, and the P–T paths are shown by arrows and lines (thick dashed line: P–T path of the pressure medium, thick solid line: that of the inclusion). At the start of an experiment, the sample chamber of the cell is loaded with an oriented quartz sample (Q), which contains a synthetic pure water inclusion. A portion of the remaining chamber volume is filled with water, which serves as the pressure medium. At low temperature (point 1), both the pressure medium and the inclusion consist of liquid water (L) and a vapor bubble (V) such that their P–T paths must follow the liquid–vapor curve of water (dotted line; cp.: critical point) when the cell is heated. At densities above the critical density of water, the vapor bubbles become smaller with increasing temperature, and eventually disappear at the homogenization temperature. Further heating causes the pressure to increase along an isochore corresponding to the water density. Measurement of the homogenization temperature is used in this study as a sensitive method to determine the densities of the pressure medium and the inclusion. At our experimental conditions, the pressure medium has a higher bulk density and therefore a lower homogenization temperature (point 2) than the inclusion (point 3). Due to its higher density, the pressure medium follows a steeper isochore than the fluid inclusion. This results in an increasing difference between the confining pressure (P_c) exerted by the pressure medium and the pressure in the inclusion (P_i). The sample is heated to a maximum temperature (point 4), left at these conditions for a short time (400 s or less), and then cooled. If deformation of the quartz around the inclusion is elastic, no change in the shape of the inclusion is observed and the P–T path of the inclusion returns to point 3. In the case of elastic behavior, the inclusion homogenization temperatures before and after heating are the same. If the stress in the quartz around the inclusion is large enough to cause plastic deformation of the host, there is a permanent change of the inclusion shape (inset at point 4; F: supercritical fluid) and the volume decreases, resulting in a rise of the inclusion pressure. In this case, the inclusion follows a different isochore upon cooling, corresponding to its new density, and has a lower homogenization temperature (point 5) than before heating (point 3).

→

free single crystal of Brazilian pegmatite quartz (0.006 wt% H). The fractures were produced by heating the core to 350°C and immersing it immediately in cold water. The starting materials were sealed in a platinum capsule, which was loaded into a cold-seal pressure vessel and run at 590°C and 200 MPa for 5 days. During that time, inclusions formed by entrapment of fluid in healed fractures in the quartz core. After run completion, the furnace was removed from the pressure vessel, which was cooled isobarically to room temperature within 4 min using an air jet. The quartz core was then removed from the capsule and cut into wafers parallel to the c-axis, which were polished on both sides to a final thickness of 80–90 μm (Fig. 2A). All inclusions in healed fractures were flat (thickness 0.5–1 μm). The inclusions selected for the experiments were relatively isolated, 20–70 μm in the longest dimension, parallel to the polished surface in their two longest dimensions, and had optically clearly discernible liquid and vapor phases. Around these inclusions, small disks with diameters of 200–300 μm were cut using a microscope-mounted cutter (U. Medenbach, Witten, Germany) so that the inclusion was approximately in the center of the disk (Fig. 2A). We only used inclusions with a minimum distance of 20 μm from the surface. This is because test experiments showed that visible brittle fractures can develop in the quartz around inclusions before the desired experimental P–T conditions are attained if the inclusions are very close (about 5 μm or less) to the surface.

Because of the nearly constant formation conditions, all inclusions had similar initial bulk densities (0.634–0.618 g/cm^3). The bulk density for each selected inclusion was determined by measuring the liquid–vapor homogenization temperature, i.e., the temperature at which the vapor phase in the inclusion disappeared upon heating (Fig. 1), and calculated from this temperature us-

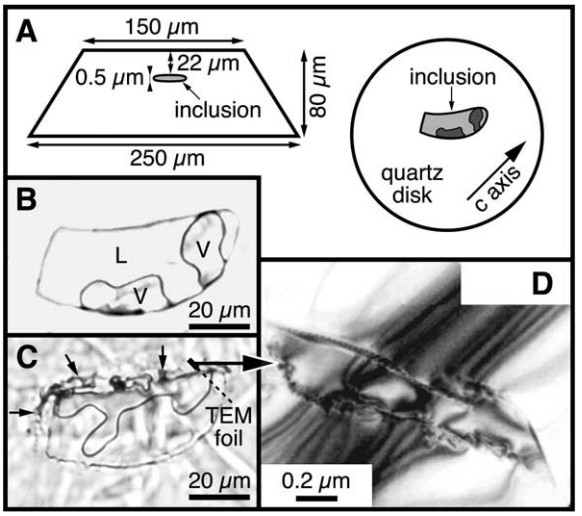

Fig. 2. (A) Example of sample and inclusion geometry. (B) Optical photomicrograph of the inclusion in A before the experiment at 25°C. L: liquid; V: vapor. (C) The same inclusion at 35°C after heating of the quartz sample to the α–β transition (728°C, 610 MPa). After less than 60 s at these conditions, the rim of the inclusion became jagged and a halo-like texture (arrows) formed rapidly in the quartz around the inclusion. Measurement of the liquid–vapor homogenization temperature of the inclusion before and after the run indicated a change in molar volume by about 7% from 28.9 to 26.9 cm^3/mol. (D) TEM image taken at the position indicated in C. Subgrains formed near the inclusion corners.

ing the equation of state of H_2O [18]. A small correction for the elastic change in inclusion volume with confining pressure P_c was applied to the determined homogenization temperature [21]. This correction is related to the change in molar volume of the quartz host, its elastic anisotropy and stress on the inclusion walls.

A schematic P–T path of the pressure medium and of an inclusion during a deformation experiment is shown in Fig. 1. During a heating experiment, the sample is monitored optically to determine P–T conditions at which permanent deformation occurs. For each sample, successive runs were performed at different P–T conditions. If no change in inclusion shape was detected within 400 s, temperature was decreased to determine if there was any change in homogenization temperatures of inclusion or pressure medium. This procedure was repeated at higher experimental temperatures and pressures until a change in shape of the inclusions was observed (Fig. 2B,C). The permanent volume change of the inclusion was confirmed by determining its density change (Fig. 1).

3. Results

Experimental conditions were chosen such that the confining pressure always exceeded the inclusion pressure. The pressure differences for the various P–T conditions at which a sample was held are shown in Fig. 3. Plastic deformation was observed as a gradual change of inclusion shape

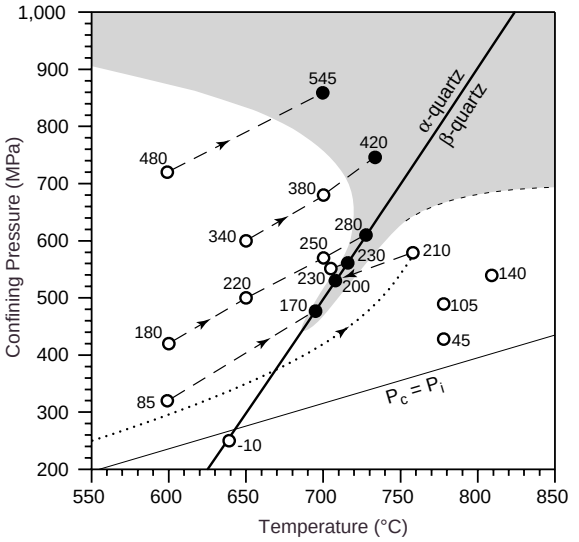

Fig. 3. P–T conditions of samples in deformation experiments. All inclusions had similar initial densities and were synthesized in the same quartz, with their two longest dimensions parallel to the crystallographic c-plane. Conditions for which the creep strength of quartz was low enough to cause short-term permanent deformation are represented by the shaded area, which shows a clear minimum of the creep strength at the α–β transition of quartz (thick black line); circles, conditions at which a sample was held (< 400 s); heavy dashed lines with arrows connect successive P–T conditions of experiments with the same inclusions; number next to circle: $P_c - P_i$ (MPa); open circles: no permanent change in density or shape of any inclusion in the sample (elastic behavior of the quartz host); filled circles: permanent change in density and/or shape of at least one inclusion in the sample (plastic deformation of quartz around inclusions); thin black line: $P_c = P_i$ (i.e., zero pressure difference) for a water density of 0.635 g/cm^3.

over tens of seconds associated with a reduction of the pressure difference but not with a full adjustment of the inclusion pressure. Plastically deformed inclusions look distinctly different (e.g., the jagged rim, Fig. 2C) from undeformed inclusions (Fig. 2B).

Within the α-quartz stability field, an irreversible shape change due to plastic deformation of the quartz around inclusions required pressure differences exceeding 400 MPa (Fig. 3). However, at the transition temperature or close to it, plastic deformation occurred at significantly lower pressure differences (170–280 MPa) within tens of seconds after the temperature was reached. To observe deformation behavior in the β-quartz stability field, the sample must be heated across the transition temperature, and since deformation occurs rapidly at the transition and at relatively low stresses, the pressure difference $P_c - P_i$ must be small enough to prevent deformation before the final run conditions are attained. A pressure difference of about 100 MPa proved to be small enough to prevent deformation when crossing the α–β boundary. However, when the sample in such an experiment was heated further along an isochore, the generated pressure difference was not large enough to cause deformation in the β-quartz stability field (open circles above 770°C, Fig. 3). We therefore allowed the *P*–*T* path of the pressure medium to deviate significantly from isochoric behavior by taking advantage of increased gasket creep with temperature (e.g., [24]) and stress applied on the gasket. This effect results in a reduction of the sample chamber volume and a corresponding increase in confining pressure (see dotted line, Fig. 3). When the sample was heated in this way to 760°C, the pressure difference after gasket creep had reached 210 MPa (as inferred from the α–β transition temperature upon isochoric cooling and the equation of state of water). At these conditions, no plastic deformation around the inclusions occurred within 5 min. However, when the sample was then cooled to the α–β transition temperature (710°C), the same inclusions deformed visibly within 1 min at a lower pressure difference of 200 MPa (Fig. 3).

After the experiments, some deformed inclusions were analyzed in detail by TEM. For this purpose, thin foils were cut from the samples around the inclusions of interest using the focused ion beam technique. This technique allows the preparation of oriented TEM foils from a precise position within the sample without damaging the material around the inclusions. TEM bright field images show dislocations and newly formed subgrains near the corners of the inclusions (Fig. 2D), where stress is most likely concentrated. In contrast, the dislocation density around undeformed inclusions is lower than observed for deformed inclusions. These observations are in agreement with previous studies on fluid inclusions [23] and imply that deformation was accommodated by the motion of dislocations.

4. Deformation mechanisms

Theoretically, several mechanisms can lead to a change in the molar volume and/or the shape of fluid inclusions in our experiments:

1. dissolution of the quartz at the inclusion–host interface and solution transfer, as quartz is quite soluble in water at elevated temperatures;
2. thermal expansion;
3. elastic compression, which is strongly anisotropic in quartz;
4. plastic flow; and
5. microcracking.

The relative effects of the first two mechanisms can be calculated based on thermodynamic data for the quartz–water system. The solubility of quartz in water is well studied [25,26] and does not show an anomaly at the α–β transition. At the conditions at which deformation was observed in the sample shown in Fig. 2 (728°C, $P_i = 330$ MPa), the solubility is about 0.3 mol SiO_2/kg H_2O [25]. This corresponds to an increase in the inclusion volume by approximately 0.5%. Solution transfer can significantly alter the shape of inclusions. However, there is no effect on the fluid density if this process occurs when only one fluid phase is present [27] as is the case in our experiments. We did observe two inclusions form from a larger inclusion by solution transfer within 5 min in an experiment in the β-quartz field at a small

pressure difference and a temperature higher than 800°C. However, these two inclusions had the same homogenization temperature (i.e., the same density) as the larger one before heating, and the new inclusions did not display the jagged rim of inclusions, which experienced permanent deformation.

Thermal expansion from the P–T conditions of inclusion homogenization to that at which deformation was observed in the sample shown in Fig. 2 ($P_c = 610$ MPa and $T = 728$°C) causes a volume increase of approximately 1% [28], but it does not change the shape of the inclusion. The anisotropic elastic decrease in inclusion volume with increasing confining pressure depends on the inclusion geometry (size and shape) and can be determined from the change in homogenization temperature with confining pressure [21]. For a number of synthetic water inclusions in our samples, we found a decrease in molar volume of 1.5% for smaller inclusions to 4% for larger inclusions for a pressure difference $P_c - P_i$ of 280 MPa, without an optically noticeable change in inclusion shape.

However, the strains caused by these three mechanisms are fully recoverable after post-experimental cooling of a sample and therefore none of them can explain the observed permanent deformation associated with an increase in the density of the fluid inclusions. Moreover, the irreversible decrease in molar volume of 7% for the inclusion shown in Fig. 2B,C is significantly larger than any of the reversible volume changes. Such an irreversible increase in density can be caused by plastic deformation of the quartz crystal around the inclusion, by diffusion of water from the pressure medium into the inclusion, or by microcracking, thus providing a path for the fluid of the confining medium to enter the fluid inclusion. The latter mechanism is ruled out as an explanation for our experimental findings for two reasons. Firstly, cracking would lead to an instantaneous adjustment of the fluid pressure in the inclusion to the confining pressure; instead we observe a gradual change of shape over tens of seconds associated with a reduction of the pressure difference but not with a full adjustment of the inclusion pressure. Secondly, visual inspection reveals no microcracks even at the TEM scale. Cracks do form visibly when the inclusion is close to the edge of the sample, at a distance of about 5 μm or less, leading to an instantaneous equilibration of the pressure. However, this is not the case in the inclusions for which results are reported here. Another potential mechanism to increase inclusion pressure without changing the inclusion shape and volume is diffusion of water through the sample. This mechanism is not relevant in our short-term experiments as water diffusion in quartz is too sluggish at these conditions [22] and we do see a shape change of the inclusions. We therefore conclude that the observed deformation around the inclusions in our quartz samples is caused by plastic deformation, in agreement with previous long-term studies [22,23]. Hence the occurrence of a relative strength minimum at the phase transition can be attributed to transformation plasticity.

5. Implications

Phase transformations in silicate rocks are ubiquitous in crust and mantle, giving rise to the consideration of transformation plasticity as the primary mechanism to localize deformation [4]. Such localized zones of low effective viscosity due to polymorphic phase transformations in the mantle could result in an instability of mantle flow [3]. Even though our observations suggest that transformation plasticity may occur in many silicate minerals, the validation of such considerations requires experimental proof of transformation plasticity of the major constituents of the mantle, in particular of olivine and its high-pressure polymorphs. By modifying the approach outlined in the study presented here, such rheologic information might well be obtained with diamond-anvil cells. For example, it was shown in previous studies with diamond-anvil cells that a non-hydrostatic stress field enhances the kinetics of the olivine to spinel phase transformation [29]. In turn the phase transformation might promote plastic deformation, similar to the transformation plasticity found in our quartz samples.

In the crust, transformation plasticity of quartz is likely to be an important mechanism to initiate localization of deformation into shear zones wher-

ever the α–β transition occurs. The transition temperature is at 574°C at room pressure and increases with pressure by 25°C/100 MPa [19]. Thus the required geological environment for the α–β transition is a warm crust, as commonly exists in tectonically active regions, for example above an ascending pluton, around metamorphic core complexes [30] or at active continental margins, such as the South American Andes, where a temperature of 800°C was inferred at a depth of 20 km [31]. In such environments, the α–β transition of quartz intersects the geothermal gradient resulting in discrete zones of much weaker crust than previously thought. This mechanism may trigger localization of deformation into these weak zones. As the mechanical response of the crust as a whole is determined by its weakest part, this conclusion is highly relevant for the dynamics of the Earth.

For fluid and melt inclusions in quartz, the consequence of a minimum in creep strength of quartz at the α–β transition is the possibility of permanent change in inclusion volume. This can occur even at laboratory timescales, as observed in our experiments. Such a permanent volume change is significant for inclusion thermobarometry, since one of the basic assumptions is that inclusions behave essentially as a constant-volume system after trapping [27]. It is known that the volume of fluid inclusions in quartz can reequilibrate during long-term geological processes [32]. Transformation plasticity is a potential mechanism to allow deformation of inclusions at much faster geological rates (e.g., cooling of igneous rocks) and has so far been overlooked.

Acknowledgements

We thank F. Schilling, B. Wunder, W. Heinrich, R. Trumbull and J. Tullis (Brown University) for stimulating discussions and critical reading of the manuscript; I. Veksler, E. Rybacki and A. Schertel (FEI, Feldkirchen) helped with preparation and analysis of the experiments. Friendly reviews by W.A. Bassett, I.-M. Chou, and an anonymous reviewer were greatly appreciated. ***[SK]***

References

[1] R.B. Gordon, Observation of crystal plasticity under high pressure with applications to the earth's mantle, J. Geophys. Res. 76 (1971) 1248–1254.
[2] C.G. Sammis, J.L. Dein, On the possibility of transformational superplasticity in the earth's mantle, J. Geophys. Res. 79 (1974) 2961–2965.
[3] E.M. Parmentier, A possible mantle instability due to superplastic deformation associated with phase transitions, Geophys. Res. Lett. 8 (1981) 143–146.
[4] J.P. Poirier, On transfomation plasticity, J. Geophys. Res. 87 (1982) 6791–6797.
[5] A. Meike, A critical review of investigations into transformation plasticity, in: J.N. Boland, J.D Fitz Gerald, (Eds.), Defects and Processes in the Solid State: Geoscience Applications, The McLaren Volume (Developments in Petrology, 14), Elsevier, Amsterdam, 1993, pp. 5–25.
[6] D.L. Kohlstedt, B. Evans, S.J. Mackwell, Strength of the lithosphere: Constraints imposed by laboratory experiments, J. Geophys. Res. 100 (1995) 17,587–17,602.
[7] R.S. Coe, M.S. Paterson, The α–β inversion in quartz: A coherent phase transition under nonhydrostatic stress, J. Geophys. Res. 74/20 (1969) 4921–4948.
[8] M.A. Carpenter, E.K.H. Salje, A. Graeme-Barber, B. Wruck, M.T. Dove, K.S. Knight, Calibration of excess thermodynamic properties and elastic constant variations associated with the α↔β phase transition in quartz, Am. Mineral. 83 (1998) 2–22.
[9] A.C.D. Chaklader, Deformation of quartz crystals at the transformation temperature, Nature 197 (1963) 791–792.
[10] G.W. Greenwood, R.H. Johnson, The deformation of metals under small stresses during phase transformations, Proc. R. Soc. London Ser. A 283 (1965) 403–422.
[11] L. Taleb, N. Cavallo, F. Waeckel, Experimental analysis of transformation plasticity, Int. J. Plast. 17/I (2001) 1–20.
[12] A.C. McLaren, A. Meike, Transformation plasticity in single and two-component ionic polycrystals in which only one component transforms, Phys. Chem. Miner. 23 (1996) 439–451.
[13] D.C. Dunand, C. Schuh, D.L. Goldsby, Pressure-induced transformation plasticity of H_2O ice, Phys. Rev. Lett. 86/4 (2001) 668–671.
[14] F.C. Luan, M.S. Paterson, Preparation and deformation of synthetic aggregates of quartz, J. Geophys. Res. 97/1 (1992) 310–320.
[15] G.C. Gleason, J. Tullis, A flow law for dislocation creep of quartz aggregates determined with the molten salt cell, Tectonophysics 247 (1995) 1–23.
[16] S.H. Kirby, The effects of the α–β phase transformation on the creep properties of hydrolytically weakened synthetic quartz, Geophys. Res. Lett. 4 (1977) 97–100.
[17] W.A. Bassett, A.H. Shen, M. Bucknum, I.-M. Chou, A new diamond anvil cell for hydrothermal studies to 2.5 GPa and from −190 to 1200°C, Rev. Sci. Instr. 64 (1993) 2340–2345.
[18] L. Haar, J.S. Gallagher, G.S. Kell, NBS/NRC Steam Ta-

bles: Thermodynamic and Transport Properties and Computer Programs for Vapor and Liquid States of Water in SI Units, Hemisphere, Washington, DC, 1984, 320 pp.
[19] A.H. Shen, W.A. Bassett, I.-M. Chou, The α-β quartz transition at high temperatures and pressures in a diamond-anvil cell by laser interferometry, Am. Mineral. 78 (1993) 694–698.
[20] R.J. Bodnar, S.M. Sterner, Synthetic fluid inclusions, in: G.C. Ulmer, H.L. Barnes (Eds.), Hydrothermal Experimental Techniques, Wiley, New York, 1987, pp. 423–457.
[21] C. Schmidt, I.-M. Chou, W.A. Bassett, R.J. Bodnar, Microthermometric analysis of synthetic fluid inclusions in the hydrothermal diamond-anvil cell, Am. Mineral. 83 (1998) 995–1007.
[22] S.M. Sterner, R.J. Bodnar, Synthetic fluid inclusions. VII. Re-equilibration of fluid inclusions in quartz during laboratory-simulated metamorphic burial and uplift, J. Metamorph. Geol. 7 (1989) 243–260.
[23] M.O. Vityk, R.J. Bodnar, J.-C. Doukhan, Synthetic fluid inclusions. XV. TEM investigation of plastic flow associated with reequilibration of fluid inclusions in natural quartz, Contrib. Mineral. Petrol. 139 (2000) 285–297.
[24] C. Schmidt, M.A. Ziemann, In-situ Raman spectroscopy of quartz: A pressure sensor for hydrothermal diamond-anvil cell experiments at elevated temperatures, Am. Mineral. 85 (2000) 1725–1734.
[25] G.M. Anderson, C.W. Burnham, The solubility of quartz in supercritical water, Am. J. Sci. 263 (1965) 494–511.
[26] C.E. Manning, The solubility of quartz in H2O in the lower crust and upper mantle, Geochim. Cosmochim. Acta 58 (1994) 4831–4839.
[27] E. Roedder, Fluid Inclusions, Reviews in Mineralogy 12, Mineralogical Society of America, Washington, DC, 1984, 646 pp.
[28] K.R. Hosieni, R.A. Howald, M.W. Scanlon, Thermodynamics of the lambda transition and the equation of state of quartz, Am. Mineral. 70 (1985) 782–793.
[29] T.-C. Wu, W.A. Bassett, P.C. Burnley, M.S. Weathers, Shear-promoted phase transitions in Fe_2SiO_4 and Mg_2SiO_4 and the mechanism of deep earthquakes, J. Geophys. Res. 98 (1993) 19,967–19,776.
[30] J. Reinhardt, U. Kleemann, Extensional unroofing of granulitic lower crust and related low-pressure, high temperature metamorphism in the Saxonian Granulite Massif, Germany, Tectonophysics 238 (1994) 71–94.
[31] J. Arndt, T. Bartel, E. Scheuber, F. Schilling, Thermal and elastic properties of crustal rocks from the central Andes, Tectonophysics 271 (1997) 75–88.
[32] M. Küster, B. Stöckhert, Density changes of fluid inclusions in high-pressure low-temperature metamorphic rocks from Crete: A thermobarometric approach based on the creep strength of the host minerals, Lithos 41 (1997) 151–167.